PAIRING MATRIX ELEMENTS AND PAIRING GAPS WITH BARE, EFFECTIVE AND INDUCED INTERACTIONS

F. Barranco[1], P.F. Bortignon[2,3], R.A. Broglia[2,3,4], G. Colò[2,3], P. Schuck[5], E. Vigezzi[3] and X. Viñas[6]

[1] Departamento de Fisica Aplicada III, Escuela Superior de Ingenieros, Universidad de Sevilla, Camino de los Descubrimientos s/n, 41092 Sevilla, Spain

[2] Dipartimento di Fisica, Università degli Studi, via Celoria 16, 20133 Milano, Italy

[3] INFN Sezione di Milano, via Celoria 16, 20133 Milano, Italy

[4] The Niels Bohr Institute, University of Copenhagen, Blegdamsvej 17, 20100 Copenhagen Ø, Denmark

[5] Institut de Physique Nucléaire, 15 rue Georges Clémenceau, 91406 Orsay Cedex, France

[6] Departament d'Estructura i Constituents de la Matèria, Facultat de Fìsica, Universitat de Barcelona, Diagonal 647, 08028 Barcelona, Spain

Abstract

The dependence on the single-particle states of the pairing matrix elements of the Gogny force and of the bare low-momentum nucleon-nucleon potential v_{low-k} - designed so as to reproduce the low-energy observables avoiding the use of a repulsive core - is studied in the semiclassical approximation for the case of a typical finite, superfluid nucleus (^{120}Sn). It is found that the matrix elements of v_{low-k} follow closely those of v_{Gogny} on a wide range of energy values around the Fermi energy e_F, those associated with v_{low-k} being less attractive. This result explains the fact that around e_F the pairing gap Δ_{Gogny} associated with the Gogny interaction (and with a density of single-particle levels corresponding to an effective k-mass $m_k \approx 0.7m$) is a factor of about 2 larger than Δ_{low-k}, being in agreement with Δ_{exp}= 1.4 MeV. The exchange of low-lying collective surface vibrations among pairs of nucleons moving in time-reversal states gives rise to an induced pairing interaction v_{ind} peaked at e_F. The interaction $(v_{low-k} + v_{ind})Z_\omega$ arising from the renormalization of the bare nucleon-nucleon potential and of the single-particle motion ($\omega-$mass

and quasiparticle strength Z_ω) due to the particle-vibration coupling leads to a value of the pairing gap at the Fermi energy Δ_{ren} which accounts for the experimental value.

An important question which remains to be studied quantitatively is to which extent Δ_{Gogny}, which depends on average parameters, and Δ_{ren}, which explicitly depends on the parameters describing the (low-energy) nuclear structure, display or not a similar isotopic dependence, and whether this dependence is born out by the data.

1 Introduction

An economic description of pairing correlations in finite nuclei is provided by Hartree-Fock-Bogoliubov (HFB) theory [1, 2] making use of phenomenological interactions like e.g. the finite range Gogny force [3] or density dependent zero-range forces combined with appropriate energy cut-offs (cf., e.g., [4, 5]). Such a description leads to values of the pairing gap which are in overall agreement with the experimental findings. Note that in these calculations, the density of levels at the Fermi energy $\rho(e_F)$ is controlled by the so called $k-$mass (i.e. $\rho(e_F) \sim m_k$) which, as a rule, is smaller than the bare nucleon mass (e.g. $m_k \approx 0.7m$ in the case of the Gogny force).

On the other hand, a number of studies have shown that the superfluid properties of nuclear systems, ranging from infinite nuclear and neutron matter to finite atomic nuclei, are strongly influenced by polarization phenomena [6]. In these calculations one starts from a bare nucleon-nucleon potential (Argonne, Bonn, Paris, etc.) adding afterwards the renormalization processes. Recently, the pairing gap, the quasiparticle spectrum and the collective modes of ^{120}Sn have been calculated solving the Dyson-Gor'kov equation [7], in a single-particle space characterized by $m_k = 0.7m$, allowing the nucleons to interact in the $^1S_0$ channel through a v_{14} Argonne N-N potential taking into account the variety of renormalization processes (self-energy, fragmentation, induced interaction and vertex corrections) arising from the coupling of the particles with surface vibrations. While the bare N-N interaction accounts for about half of the pairing gap, overall agreement with the experimental findings is achieved by including medium polarization effects.

In the present paper we want to shed light into the physics of these results, by studying the magnitude of the different pairing ($J^\pi = 0^+$) matrix elements as well as their dependence on the energy of the single-particle states lying in the vicinity of the Fermi energy in Section 2, and by discussing the calculation of the pairing gaps associated with these matrix elements in Section 3.

2 Matrix elements

The matrix element of the induced interaction can be written as [8]

$$\langle \nu' \bar{\nu}' | v_{ind} | \nu, \bar{\nu} \rangle = 2 \sum_{LMn} \frac{< \nu | f_{Ln} Y_{LM} | \nu' >< \bar{\nu} | f_{Ln} Y^*_{LM} | \bar{\nu}' >}{E_0 - |e_\nu - e_F| - |e_{\nu'} - e_F| - \hbar\omega_{Ln}}, \qquad (1)$$

where L, M and n denote the quantum numbers of the exchanged collective vibrations, $f_{Ln}(r) = \beta_{Ln} R_0 (dU/dr)$ is the associated radial formfactor (β_{Ln} is the deformation parameter associated with the $n-$th mode of multipolarity L, R_0 is the ground-state radius and U is the average potential), $\hbar\omega_{Ln}$ is the vibrational energy of the $n-$th mode, while e_ν and e_F are the single-particle and Fermi energies. E_0 is the pairing correlation energy per Cooper pair, which is of the order of $-\Delta$. In practice we have used E_0= - 2 MeV. The pre-factor 2 in Eq. (1) comes from the two possible time orderings associated with the one-phonon exchange.

In Fig. 1 we show the value of the diagonal matrix elements $\langle \nu\bar{\nu} | v_{ind} | \nu\bar{\nu} \rangle$ of the induced interaction for the nucleus ^{120}Sn as a function of the single-particle energy. The single-particle levels entering Eq. (1) have been calculated making use of a standard Saxon-Woods potential, whose parameters are provided in the caption of Fig. 1. In most of our calculations we use this potential and an associated effective mass m_k equal to the bare mass. In the last section we shall use instead an effective mass $m_k = 0.7m$, which simulates the typical outcome of a Hartree-Fock calculation (with, e.g., the Gogny interaction). In those cases, the Woods-Saxon parameters are changed in such a way that the Fermi energy remains close to the experimental value ($V_0^{'}$ $\approx (m/m_k)V_0$ [9], see e.g. Fig. 8). The parameters β_{Ln} and $\hbar\omega_{Ln}$ have been determined by diagonalizing a separable multipole-multipole interaction in the quasiparticle-random phase approximation (QRPA) adjusting the coupling constants so as to reproduce the energies and transition probabilities of the lowest-lying states of each spin and parity. Also shown in Fig. 1 are

the diagonal matrix elements of the Gogny interaction. Here, and in the rest of the paper, we shall employ the D1 parametrization.

The matrix elements of v_{ind}, which display an average value equal to -0.15 MeV, are peaked at the Fermi energy, within an energy range of essentially 5 MeV around e_F. This behaviour reflects the fact that $\langle \nu' \bar{\nu}' | v_{ind} | \nu, \bar{\nu} \rangle$ is controlled, through the energy denominator appearing in Eq.(1), by the energy of the low-lying collective vibrations ($\hbar\omega_L(n) < 5$ MeV). Outside this energy range, the values of $\langle \nu' \bar{\nu}' | v_{ind} | \nu, \bar{\nu} \rangle$ become very small, less than 50 keV in absolute value. The matrix elements of v_{Gogny} decrease on average smoothly in magnitude all the way from the deepest levels up to the continuum threshold, displaying a value of about -0.3 MeV at e_F.

The induced interaction matrix elements depend on specific properties of finite nuclei, namely the single-particle quantum numbers and energies, and the energy, the zero-point amplitude and the transition density of the vibrational states. To study the global features of the bare, of the induced, and of the Gogny interactions as well as to provide a more transparent form for their matrix elements, we shall present, in the rest of this section, also the matrix elements obtained using the semiclassical Thomas-Fermi (TF) approximation. In fact, this approximation averages out shell effects typical of finite nuclei and provides the overall energy dependence of the matrix elements. Within this context we follow Ref. [10] where semiclassical expressions for two-body matrix elements have been presented. To obtain a smooth behaviour of the diagonal matrix elements as a function of the continuous energy variable E, we compute the Fourier transform of a two-body interaction $v(\vec{r}_1, \vec{r}_2)$ using plane waves of momenta $\vec{p}_1$ and $\vec{p}_2$. The average of the quantal matrix elements is carried out using the normalized semiclassical density matrix,

$$\rho_E = \frac{1}{g(E)} \delta(E - H_{cl}) = \frac{1}{g(E)} \delta(E - \frac{p2}{2m_k} - U(r)). \tag{2}$$

In the above relation the semiclassical level density g is

$$g(E) = \frac{1}{\pi} \int_0^{R_c} dr r^2 (\frac{2m_k}{\hbar^2})^{3/2} \sqrt{E - U(r)}, \tag{3}$$

R_c being the classical turning point. We assume a constant value for the effective mass m_k, neglecting its possible dependence on position. The expression for the semiclassical diagonal matrix element of $v(\vec{r}_1, \vec{r}_2)$ as a function of the

single-particle energy, is consequently [10]

$$v(E) = \int d^3r_1 d^3r_2 v(\vec{r}_1, \vec{r}_2) \times$$
$$\times \int \frac{d^3p_1 d^3p_2}{(2\pi\hbar)^6} \frac{e^{\frac{i}{\hbar}(\vec{p}_1 - \vec{p}_2)\vec{s}}}{g^2(E)} \delta(E - \frac{p_1^2}{2m_k} - U(r_1))\delta(E - \frac{p_2^2}{2m_k} - U(r_2)). \quad (4)$$

For an interaction that depends only on the magnitude of the relative coordinate $s \equiv \vec{r}_1 - \vec{r}_2$, like the Gogny interaction in the S=0, T=1 channel, one can integrate first over d^3s and then over the momenta d^3p_1 and d^3p_2, obtaining the expression

$$v(E) = c(E) \int d^3R (E - U(R))\theta(E - U(R)) v(k_E(R), k_E(R)), \quad (5)$$

where R indicates the center of mass, $v(k,k)$ is the on-shell pairing matrix element of the interaction $v(s)$ in the ${}^1S_0$ channel and in a plane wave basis, evaluated at the local momentum $k = k_E(R) = \frac{1}{\hbar}\sqrt{2m_k(E - U(R))}$, and $c(E)$ denotes the quantity

$$c(E) = \frac{2{m_k}^3}{4\pi^4\hbar^6 g^2(E)}. \quad (6)$$

In the next section we shall calculate the pairing gap associated with the different interactions, and therefore we shall need the matrix elements between all pairs of particles moving in time reversal. For this purpose we shall employ a formula analogous to that given in Eq. (5), namely

$$v(E, E') = \sqrt{c(E)c(E')} \int d^3R \sqrt{(E - U(R))}\sqrt{(E' - U(R))} \times$$
$$\times \theta(E - U(R))\theta(E' - U(R)) v(k_E(R), k_{E'}(R)). \quad (7)$$

In this relation E and E' indicate the energies of the single-particle states of each pair.

We now turn to the case of the induced interaction, associated with the matrix elements of Eq. (1). In this case the matrix elements depend separately on $\vec{r}_1$ and $\vec{r}_2$. We then integrate over the momenta first, obtaining

$$v_{ind}(E) = 2 \sum_{nLM} c(E) \frac{\int d^3r_1 d^3r_2 f_{Ln}(r_1) Y_{LM}(\hat{r}_1) f_{Ln}(r_2) Y^*_{LM}(\hat{r}_2) j_0^2(ks)(E - U(R))}{E_0 - 2|E - e_F| - \hbar\omega_{nL}}, \quad (8)$$

where j_0 is the Bessel function and $k \equiv \sqrt{\frac{2m_k}{\hbar^2}(E - U(R))}$. The index n labels the different phonons of multipolarity L (the phonons included in the present calculation are specified at the end of this Section). Note that one can obtain numerical results from Eq. (8) by avoiding the six-dimensional integration. This is achieved by performing a multipole expansion of the quantity

$$j_0^2(ks)(E - U(R)) = \sum_{lm} \frac{4\pi}{2l+1} F_l(r_1, r_2; E) Y_{lm}(\hat{r}_1) Y^*_{lm}(\hat{r}_2),$$

which leads to

$$v_{ind}(E) = 2 \sum_{nL} 4\pi c(E) \frac{\int dr_1 dr_2 r_1^2 r_2^2 f_{Ln}(r_1) f_{Ln}(r_2) F_L(r_1, r_2; E)}{E_0 - 2|E - e_F| - \hbar\omega_{Ln}}. \qquad (9)$$

In Ref. [10] the reliability of the TF approximation in reproducing the quantum mechanical (QM) matrix elements has been checked in the particular case of the pairing matrix elements of a δ-interaction acting among particles moving in a harmonic oscillator (HO) potential. Note that the TF approach implies an averaging over the quantum numbers associated with the different states belonging to the major shells and displaying an energy $E_N = (N + \frac{3}{2})\hbar\omega$. The TF matrix elements have been compared with the averaged QM matrix elements (taking degeneracies into account). Overall agreement was observed (cf. Table II of Ref. [10]).

A similar comparison for the pairing matrix elements of the Gogny force in the $^1S_0$ channel is reported in Fig. 2. It is seen that the TF approach provides a good approximation to the average quantum matrix elements. However, the QM diagonal matrix elements, in particular those associated with s-states, are systematically larger (in absolute value) than the non-diagonal ones. One should be aware of the fact that the semiclassical density matrix can be considered to be the analogue to the one obtained from a Strutinsky smoothing. Therefore, Eq. (2), implicitly, represents a function of about $1\hbar\omega$ width. Thus, the matrix element in Eq. (4) contains at the quantum level cross terms corresponding to at least one major shell. Taking for example the 2s-1d shell, we have to weigh the two diagonal matrix elements with the 2s and 1d wavefunctions with a factor 1 and 25, respectively. The non-diagonal 2s-1d element obtains the weight factor 10. Performing the arithmetic average yields the crosses of Fig. 2. In this way, we see that the TF expression (4) reproduces very well the quantal average. The more realistic case of the Gogny matrix elements in the Woods-Saxon potential (including spin-orbit)

is illustrated in Fig. 3. The general pattern is similar to that shown in the previous figure.

Having assessed its validity, we now employ the semiclassical approximation to compare the matrix elements of the induced interaction, the effective Gogny interaction and a bare nucleon-nucleon interaction. Concerning the latter, the matrix elements of bare nucleon-nucleon interactions which contain a repulsive core display a qualitatively different momentum dependence than that displayed by the Gogny interaction. We shall instead consider here the v_{low-k} interaction, which has been devised to reproduce the low-momentum properties of the nucleon-nucleon force, including the experimental phase shifts, without the introduction of a repulsive core [11]. In particular, we shall employ a parametrization of v_{low-k} devised to reproduce the properties of v_{14} Argonne potential. This parametrization requires a momentum cutoff k_{cut} equal to 2.1 fm^{-1}. The matrix elements of v_{low-k} in a plane wave basis have been calculated in Ref. [12] and are reported in Fig. 4. It is seen that, while v_{Gogny} is less attractive than v_{low-k} for small momenta, it becomes more attractive for k larger than $\approx$1 fm^{-1}.

The semiclassical matrix elements of the Gogny D1 interaction (Eq. (5)) and of the v_{low-k} interactions calculated as a function of the single-particle energy for the nucleus ^{120}Sn, are displayed in Fig. 5. We remark that, close to the Fermi energy, the matrix elements of the Gogny interaction calculated with the D1S parametrization are about 10 keV less attractive. It is seen that the general trend is the same as that obtained in infinite matter, with the difference that the matrix elements of the two interactions look somewhat more similar to one another. Insight into this difference can be obtained with the help of Eq.(5). This relation is essentially an average of $v(k)$ calculated at the various local momenta in the nucleus. From Fig. 4 we see that in the interior of the nucleus (at larger local momenta) v_{Gogny} is more attractive than v_{low-k}, but on the surface it tends to be less attractive than v_{low-k}.

The semiclassical matrix elements of the induced interaction are also shown in Fig. 5. These matrix elements are strongly peaked around the Fermi energy and reproduce rather well the average of the quantal results already shown in Fig. 1. In Fig. 6 we have separated the contributions arising from the exchange of phonons of multipolarities L=2, 3 and 4. We include all the phonons with energy below 30 MeV in the calculation. The importance of the contributions with L=2 and 3 can be understood in terms of the high collectivity and low energy of the associated collective modes. The energies and deformation parameters of the low-lying modes are $\hbar\omega_2 = 1.17$ MeV ,

$\hbar\omega_3 = 2.42$ MeV, $\hbar\omega_4 = 2.47$ MeV and $\beta_2 = 0.12$, $\beta_3 = 0.15$, $\beta_4 = 0.07$.

We also note that at the Fermi energy the matrix elements of v_{ind} are rather large, of the order of those associated with the bare nucleon-nucleon potential v_{low-k} (in this connection, cf. the estimate in ref. [13]) .

3 Pairing gaps

In this section, we shall discuss the results of calculations of the pairing gap which employ the matrix elements discussed above. In the nucleus under study, namely ^{120}Sn, we obtain the state-dependent pairing gaps by solving the generalized BCS equations [14]: this means that we solve the HFB equations by treating the pairing sector self-consistently, while the mean field is described in terms of the Woods-Saxon potential already used in the calculation of the matrix elements. In this way, we take into account scattering processes between nucleons lying on orbits having different number of nodes/energies [4], associated with non-diagonal matrix elements of the type $v(E_1, E_2; E_1', E_2')$, with different energies E_1 and E_2 (or E_1' and E_2'). This is at variance with the usual BCS method in which the pairing gap receives contributions only from scattering processes between time-reversal states. We shall refer in the following either to quantal or to semiclassical calculations; in the latter case, this is done by solving the same equations as in the quantal case, but replacing the QM matrix elements with the TF ones, using Eq. (7) and the prescription

$$E = (E_1 + E_2)/2, \quad E' = (E_1' + E_2')/2. \tag{10}$$

The positive energy states are obtained by setting the system in a spherical box. We have checked that convergence is achieved using R_{box}=12 fm and including all the states from the bottom of the potential up to the positive energy E_{cut}=50 MeV.

In infinite neutron matter, the pairing gaps calculated with the interactions v_{low-k} and v_{Gogny} are very similar up to Fermi momenta of the order of 0.6 fm^{-1}, becoming increasingly different from each other at higher momenta, as can be seen from Fig. 7 (cf. Ref. [5, 12], where the D1S parametrization of the Gogny interaction has been used). The pairing gap obtained with v_{low-k} goes to zero, around saturation, as a function of k_F much faster than that associated with v_{Gogny}; it can also be seen that the pairing gap obtained

with v_{low-k} reproduces quite accurately the result found allowing particles to interact through the Argonne v_{14} bare N-N potential [15].

In the case of ^{120}Sn, the pairing gap with the v_{14} Argonne interaction and with $m_k = m$, was calculated previously in ref. [16], obtaining a value of about 2.2 MeV close to the Fermi energy. We have verified that essentially the same value is obtained with v_{low-k}, in keeping with the infinite matter case (cf. Fig. 7). In the following, however, we shall adopt the value $m_k = 0.7m$, which is the typical value associated with Hartree-Fock calculations performed with Gogny or Skyrme forces. In Fig. 8 we compare the state-dependent pairing gap obtained with the Gogny force and with the v_{low-k} interaction. We also compare the pairing gaps obtained inserting the semiclassical pairing matrix elements in the HFB equations. We remark that the semiclassical approach takes out the scatter from shell effects which is a desirable feature when one wishes to reveal generic trends.

The Gogny interaction leads to a pairing gap of 1.4 MeV close to the Fermi energy, in good agreement with the experimental value deduced from the odd-even mass difference. This value is about two times larger than that obtained with v_{low-k}. Note also that the pairing gap obtained with v_{low-k} reproduces the results obtained with the bare v_{14} interaction [7]. We remark that using the D1S parametrization of the Gogny force, instead of D1, one obtains a gap at the Fermi energy of about 1.2 MeV.

In Fig. 9 we show the state-dependent pairing gap obtained with the pairing matrix elements of $v_{total} = v_{low-k} + v_{ind}$, resulting from the sum of the matrix elements of the bare interaction v_{low-k} and of the induced interaction v_{ind}. The average value of the resulting pairing gap Δ_{total} at the Fermi energy is about 2 MeV. This value is about 25% higher than that obtained in Ref. [7], where we solved the Dyson-Gor'kov equation, taking properly into account all polarization effects (induced interaction, self-energy and vertex corrections) [17].

This is consistent with the fact that according to Nuclear Field Theory (NFT) [18], if one considers the effects of the exchange of phonons between pairs of nucleons, one has to consider at the same time processes where the phonon is absorbed by the same nucleon which has virtually excited it. Such processes lead to self-energy (ω-mass and single-particle splitting) as well as to vertex correction phenomena. Of these processes and for the nucleus under discussion (^{120}Sn), $\omega-$mass effects [9] are the most important. Taking such effects into account is equivalent to use a residual interaction $v_{ren} = v_{total} Z_\omega$, where $Z_\omega = (m_\omega/m)^{-1}$ is the quasiparticle strength [9] at

the Fermi energy (cf. Appendix A). Consequently $\Delta_{ren} = Z_\omega \Delta_{tot}$. Because v_{ind} is proportional to β_L^2/DEN_L, that is to the square of the deformation parameters associated with the low-lying collective vibration and inversely proportional to the energy denominator DEN_L appearing in Eq.(1), a typical error of 20% on β_L and DEN_L implies a 60% error in v_{ind}. Making use of this fact and of the results of Figs. 1 and 9 one obtains, as discussed in Appendix B, $\Delta_{ren} \approx Z_\omega \Delta_{tot} \approx 1.35 \pm 0.15$ MeV. It is seen that the 60% error in v_{ind} has been reduced to a 10% in Δ_{ind}. This is because the stronger the particle-vibration coupling is, the larger Δ_{tot} but the smaller the amount of single-particle content of levels around ϵ_F (and thus the smaller Z_ω), and viceversa. The self consistency between collectivity of the modes, strength of the particle-vibration coupling, and quasi-particle residue at the pole, typical of NFT, allows theory to make predictions which are more accurate than the basic parameters entering the calculation, as a result of a delicate process of cancellation of errors.

4 Conclusions

Summing up, we have found that the small difference existing between the matrix elements of the bare v_{low-k} interaction and those of the Gogny interaction leads to important differences between the pairing gaps associated with the two forces ($\Delta_{Gogny} \approx 2\Delta_{low-k}$, for $m_k \approx 0.7m$). This difference is removed and eventually overwhelmed by including the attractive contribution coming from the induced interaction v_{ind} arising from the exchange of surface vibrations, which acts only on a rather small energy range around e_F. We note that the pairing gap in ^{120}Sn is not much changed, including also the effect of spin fluctuations [22], which instead give the dominant (repulsive) contribution to the induced interaction in neutron matter.

The 25% excess displayed by the resulting total pairing gap with respect to the experimental value is corrected by considering the corresponding quasi-particle strength at the Fermi energy. An important question which remains to be addressed quantitatively is the ability $v_{low-k} + v_{ind}$ as well as v_{Gogny} have to describe in detail the isotopic and nuclear structure dependences displayed by Δ_{exp}. This subject will be addressed in a future publication.

Within this context, we note that the dependence of the pairing gaps generated by v_{Gogny} and by $v_{low-k} + v_{ind}$ on temperature and rotational frequency is expected to be quite different, as v_{Gogny} and v_{low-k} are essentially

independent of these parameters, while v_{ind} is quite sensitive to them.

It is also worth mentioning that a recent study in symmetric nuclear matter revealed a very strong extra attraction coming from the induced interaction [23]. Nuclear matter and finite nuclei may, however, show only qualitative similarities in this case and a quantitative link may be difficult to establish.

We thank L. Coraggio for providing us with the matrix elements of the v_{low-k} interaction.

References

[1] J.P. Blaizot and G. Ripka, *Quantum theory of finite systems*, The MIT Press (1985).

[2] P. Ring and P. Schuck, *The nuclear many-body problem*, Springer-Verlag (1980).

[3] J. Dechargé and D. Gogny, Phys. Rev. **C21** (1980) 1668.

[4] T. Duguet, P. Bonche, P.-H. Heenen, J. Meyer, Phys. Rev. **C65** (2002) 014311; J. Dobaczewski, W. Nazarewicz, T.R. Werner, J.F. Berger, C.R. Chinn, J. Dechargé, Phys. Rev. **C53** (1996) 2809.

[5] E. Garrido, P. Sarriguren, E. Moya de Guerra, P. Schuck, Phys. Rev. **C60** (1999) 064312; E. Garrido, P. Sarriguren, E. Moya de Guerra, U. Lombardo, P. Schuck, H.J. Schulze, Phys. Rev. **C63** (2001) 037304.

[6] U. Lombardo and H.-J. Schultze, in *Physics of neutron star interiors*, eds. D. Blaschke, N.K. Glendenning and A. Sedrakian, Springer (2001), p.30.

[7] F. Barranco, R.A. Broglia, G. Colò, E. Vigezzi and P.F. Bortignon, Eur. Phys. J. **A21** (2004) 57.

[8] F. Barranco, R.A. Broglia, G. Gori, E. Vigezzi, P.F. Bortignon, J. Terasaki, Phys. Rev. Lett. **83** (1999) 2147.

[9] C.Mahaux, P.F. Bortignon, R.A. Broglia, C. H. Dasso, Phys. Rep. **120** (1985) 1.

[10] X. Viñas, P. Schuck, M. Farine and M. Centelles, Phys. Rev. **C67** (2003) 054307.

[11] L. Coraggio, A. Covello, A. Gargano, N. Itaco, T.T.S. Kuo, Phys. Rev. **C66** (2002) 064311.

[12] A. Sedrakian, T.T.S. Kuo, H. Müther and P. Schuck, Phys. Lett. **B576** (2004) 68.

[13] A. Bohr and B.R. Mottelson, *Nuclear Structure*, Vol. II, Benajmin (1975), p. 432.

[14] F. Barranco, R.A. Broglia, H.Esbensen, E. Vigezzi, Phys.Rev. **C58**(1998)1257.

[15] A. Schwenk, B. Friman, G.E. Brown, Nucl. Phys. **A713**(2003) 191.

[16] F. Barranco, R.A. Broglia, H. Esbensen and E. Vigezzi, Phys. Lett. **B390** (1997) 13.

[17] J. Terasaki, F. Barranco, R.A. Broglia, E. Vigezzi, P.F. Bortignon, Nucl. Phys. **A697**(2002) 127.

[18] D. R. Bes, R.A.Broglia, G. G. Dussel, R. J. Liotta and H. M. Sofia, Nucl. Phys. **A260** (1976) 1; ibid., 27; D. R. Bes, R.A.Broglia, G. G. Dussel, R. J. Liotta and R. J. Perazzo, Nucl. Phys. **A260** (1976) 77;

[19] D. Brink and R.A. Broglia, *Nuclear supefluidity: pairing in finite systems*, Cambridge University Press, Cambridge (2005).

[20] A. Bohr and B.R. Mottelson, *Nuclear Structure*, vol I, Benjamin (1969).

[21] J.R. Schrieffer, *Superconductivity*, Benjamin, New York (1964).

[22] G. Gori et al., to be published.

[23] C. Shen et al., to be published.

Appendix A

Simple estimate of the pairing gap

In what follows we consider some of the consequences the particle-vibration coupling has on the pairing correlations of particles moving in a single j-shell interacting through a bare nucleon-nucleon pairing potential with constant matrix elements G [19].

For this simple model, the value of the occupation numbers U_ν and V_ν must be the same for all the $2j+1$ orbitals. In particular, the occupation probability for the case when the system is occupied with $N = \Omega$ particles (half filled shell), where

$$\Omega = \frac{2j+1}{2} \tag{A.1}$$

is

$$V = \sqrt{\frac{N}{2\Omega}} = \sqrt{\frac{1}{2}}, \tag{A.2}$$

$$U = \sqrt{1 - \frac{N}{2\Omega}} = \sqrt{\frac{1}{2}}. \tag{A.3}$$

Consequently, the pairing gap is given by the relation

$$\Delta = G \sum_{\nu>0} U_\nu V_\nu = \frac{G\Omega}{2}. \tag{A.4}$$

Because the density of levels is proportional to the $\omega-$mass (m_ω), the effective (dressed) degeneracy can be written

$$\Omega_{eff} = \frac{\Omega}{Z_\omega}, \tag{A.5}$$

in terms of the quasiparticle strength at the Fermi energy $Z_\omega = (m_\omega/m)^{-1}$ where $m_\omega = m(1+\lambda)$, λ being the mass enhancement factor. In the case of nuclei this dimensionless quantity (which measures the strength with which nucleons couple to low-lying collective vibrations) is of the order of 0.5, closer to the strong than to the weak coupling situation of BCS (in which case $\Delta \sim \lambda$) [21].

Because of their coupling to vibrations, nucleons spend part of the time in more complicated configurations than pure single-particle states. The quantity (quasiparticle strength [9]) $Z_\omega = (1+\lambda)^{-1} \approx 0.7$ measures the content of single-particle strength present in levels around the Fermi energy available for nucleons to interact through a two-body interaction, in particular through through a pairing force. Consequently, due to the self-energy processes arising from the particle-vibration coupling phenomenon, the pairing strength becomes $G{Z_\omega}^2$.

The exchange of vibrations between pairs of nucleons moving in time reversal states close to the Fermi energy gives rise to an effective pairing interaction of strength $g_{p-v}{Z_\omega}^2$, where g_{p-v} stands for the induced pairing interaction controlled by the particle-vibration coupling vertices. Taking these effects into account, one can write

$$\Delta = \frac{Z_\omega}{2}(G + g_{p-v})\Omega \tag{A.6}$$

Identifying G with v_{low-k} and g_{p-v} with v_{ind}, one finds from Fig. 9 that

$$\frac{1}{2}(G + g_{p-v})\Omega \approx 2\text{MeV}. \tag{A.7}$$

As seen from Eq. (A.6), the number to be compared with experimental findings is

$$\Delta_{ren} = Z_\omega \times 2\text{MeV} \approx 1.4\text{MeV}. \tag{A.8}$$

Note that in the above discussion we have not considered the errors to be expected in estimating both g_{p-v} and Z_ω. This subject is taken up in Appendix B.

Appendix B

Simple estimate of λ and Z_ω

From Fig. 1 it is seen that the average values of v_{ind} and v_{low-k} at the Fermi energy are $< v_{ind} >$ = -0.15 MeV and $< v_{low-k} >$ = -0.16 MeV. Because v_{ind} is of the order of $\sum_L \beta_L^2 / DEN_L$, the matrix elements of v_{ind} will display an error equal to twice the average error displayed by β_L plus that displayed by DEN_L. Assuming this error to be 20% for both quantities (a rather extreme negative situation) one concludes that $< v_{ind} >= 0.15 \pm 0.09$ MeV. Consequently $< v_{tot} >=< v_{ind} > + < v_{low-k} >= -0.31 \pm 0.09$ MeV. Because Δ_{total} = 2 MeV for $< v_{tot} >$ = -0.31 MeV, one obtains $\Delta_{total} = (2 \pm 0.6)$ MeV.

We now proceed to the calculation of $\lambda = N(0) < v_{ind} >$, where $N(0)$ is the density of single-particle levels around the Fermi energy for one spin orientation and one type of nucleon. Making use of the value $N(0) = 3.4$ MeV^{-1} appropriate for ^{120}Sn, one gets $\lambda = 0.5 \pm 0.3$. Consequently $\Delta_{ren} = Z_\omega \Delta_{tot}$ = 1.35 $\pm$ 0.15 MeV, where $Z_\omega = (1 + \lambda)^{-1}$. We thus note a conspicuously smaller error for Δ_{ren} than for v_{ind}. This is because the larger is λ (induced pairing contribution), the smaller is the content of single-particle strength and thus of Z_ω, associated with levels lying close to the Fermi energy, and viceversa.

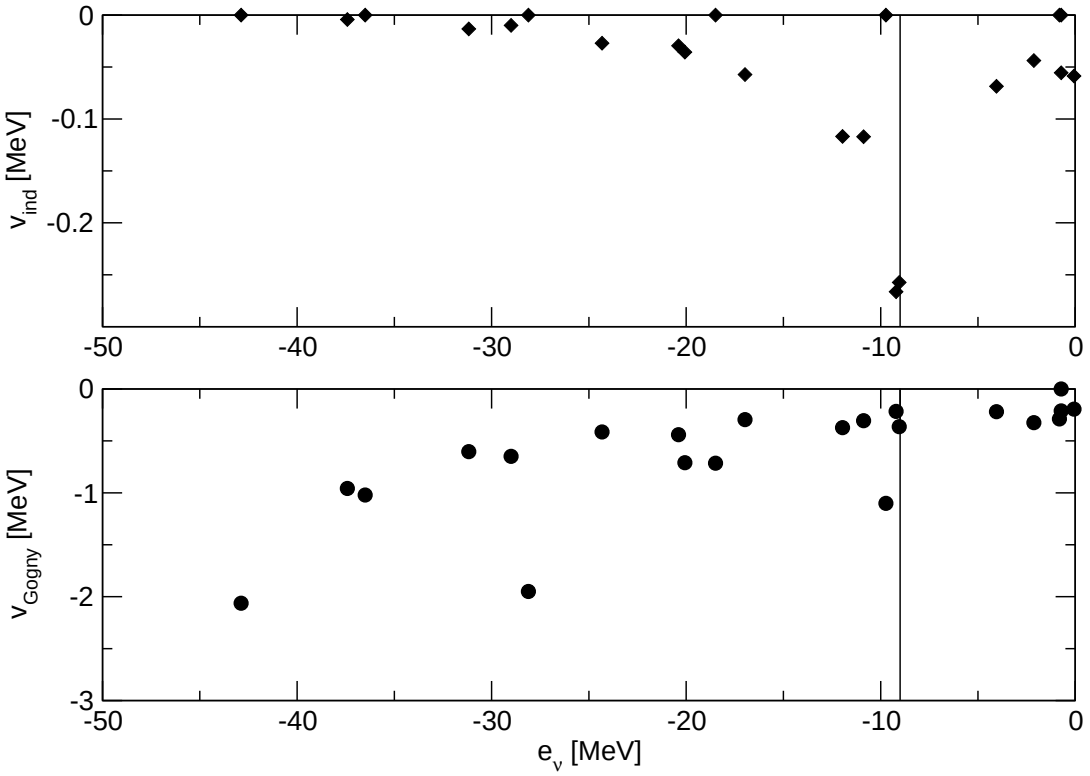

Figure 1: The nucleus ^{120}Sn. Diagonal pairing matrix elements of the induced interaction (upper panel, solid diamonds) and of the Gogny force (lower panel, solid circles), displayed as a function of the single-particle energy e_ν of the state ν calculated using the bare nucleon mass and the single-particle wavefunctions of a Woods-Saxon potential with standard parameters (depth V_0= -49 MeV, diffusivity a =0.65 fm, and radius $R_0 = 6.16$ fm), including the spin-orbit term, parametrized according to ref. [20]. Also shown by means of vertical lines is the position of the Fermi energy, $e_F = -9.1$ MeV. Note the different scale in the two figures.

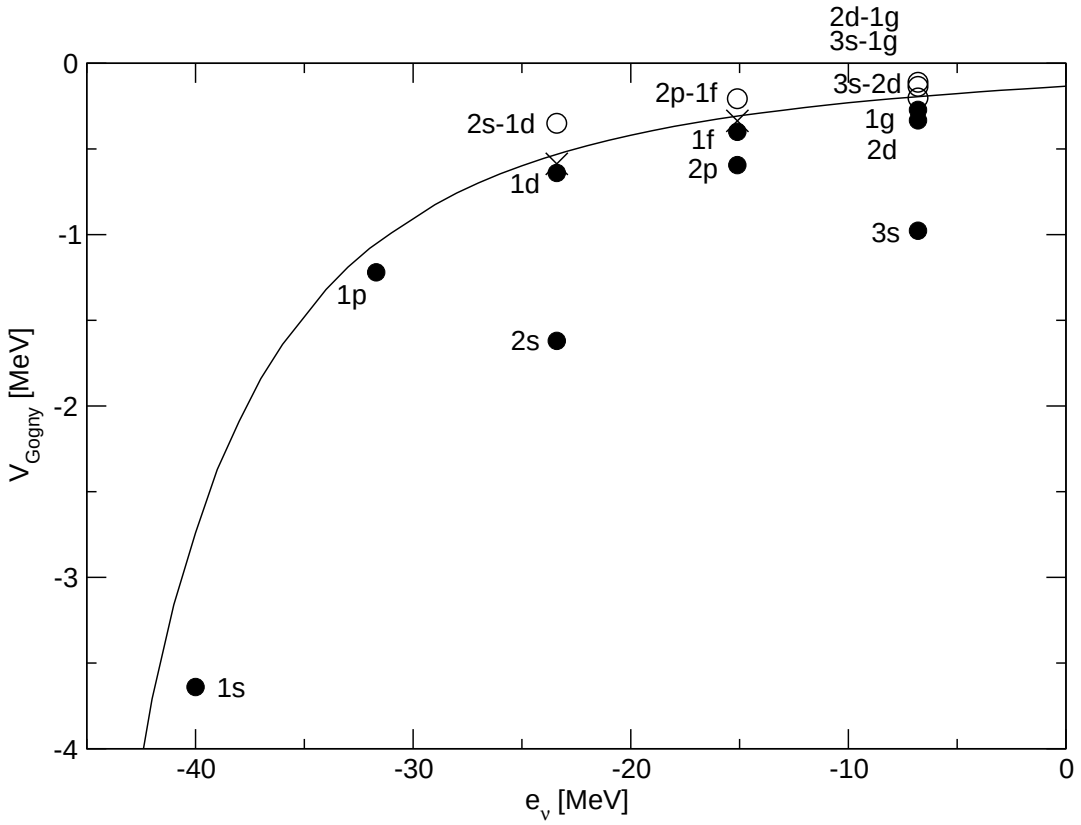

Figure 2: Schematic model for the nucleus ^{120}Sn. The semiclassical pairing matrix elements of the Gogny force (solid line) are compared to the quantal matrix elements for the case in which the single-particle wavefunctions have been calculated making use of a harmonic oscillator potential without the spin-orbit term (and $m_k = m$). The diagonal and non-diagonal matrix elements are denoted by filled and open circles respectively. The crosses correspond to the weighted averages of the matrix elements within a shell.

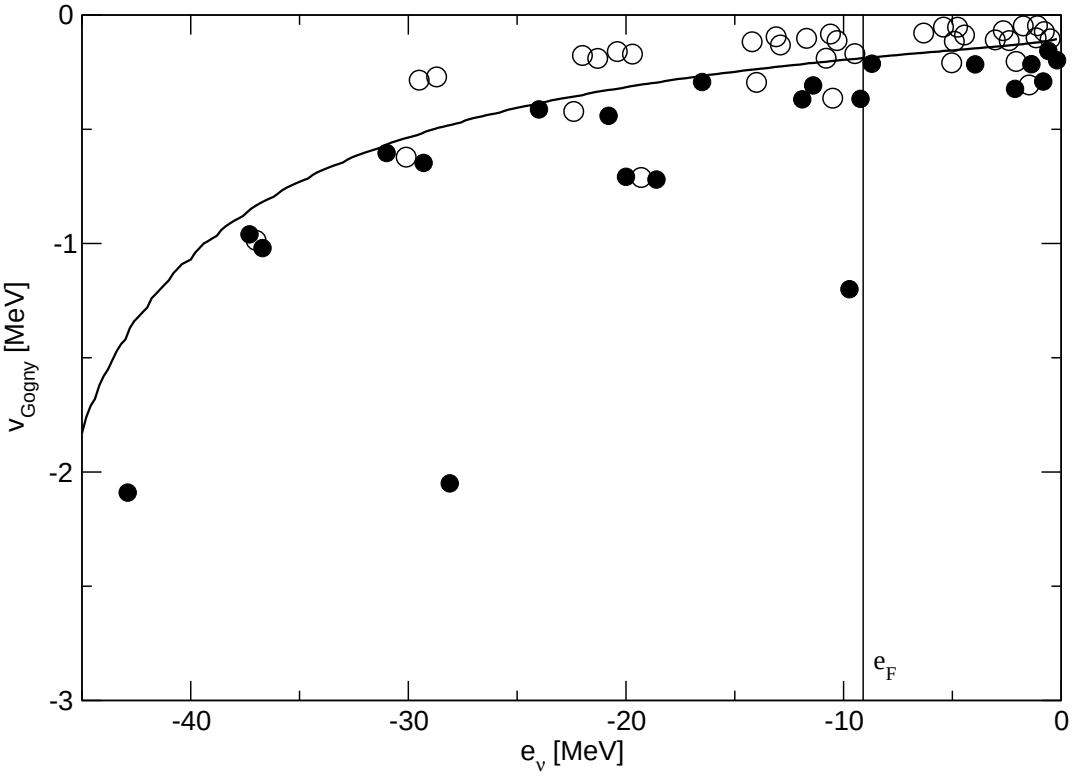

Figure 3: The nucleus ^{120}Sn. The same as Fig. 2 (i.e. also with $m_k = m$) but for the fact that the single-particle wavefunctions have been calculated making use of the Woods-Saxon potential including the spin-orbit term already used for Fig. 1, where the diagonal matrix elements have already been shown. The non-diagonal matrix elements are plotted here at an energy e_ν which is the average between the energies of the initial and final states.

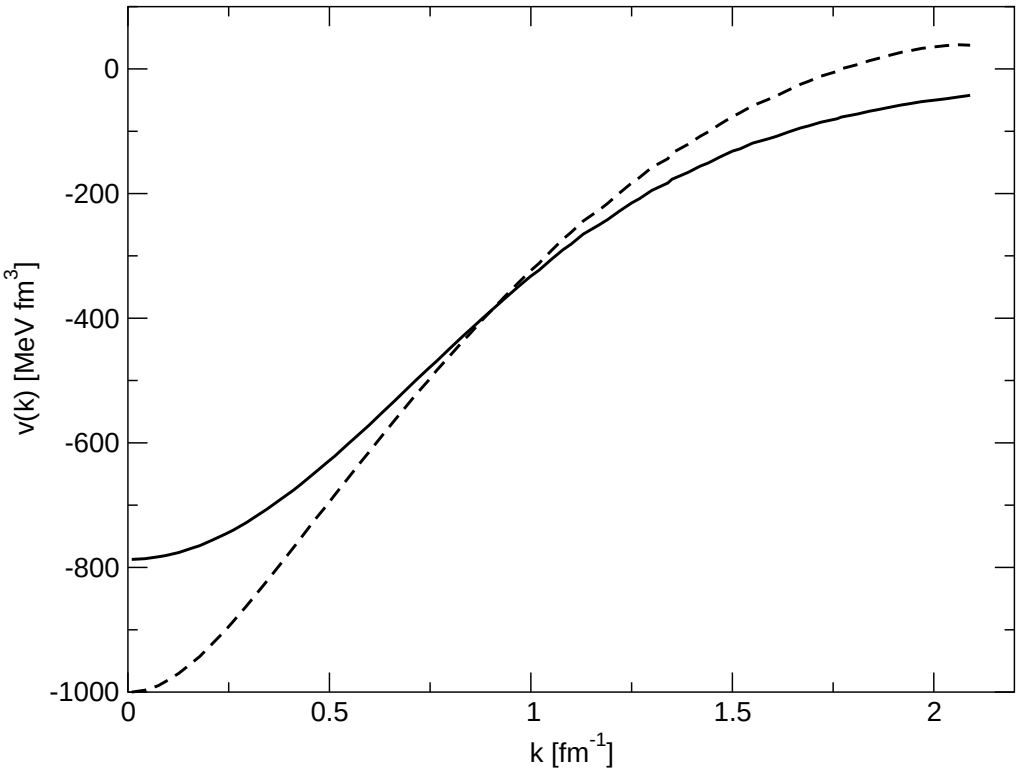

Figure 4: The matrix elements of the Gogny (solid curve) and of the v_{low-k} (dashed curve) interactions are plotted as a function of momentum.

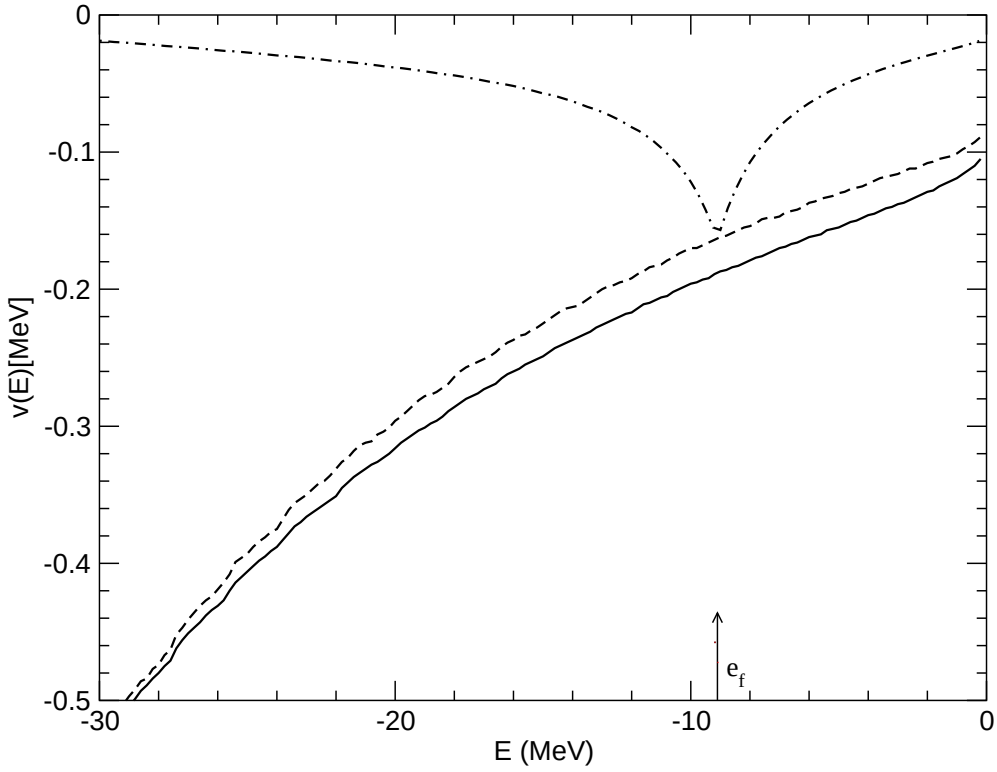

Figure 5: The nucleus ^{120}Sn. The semiclassical matrix elements of the induced interaction, calculated according to Eq. (9)(dash-dotted curve), are compared with the matrix elements of the Gogny force (solid curve, cf. Fig. 3) and with those of the v_{low-k} interaction (dashed curve). Calculations are performed with $m_k = m$ and with the same Woods-Saxon potential used in Figs. 1 and 3.

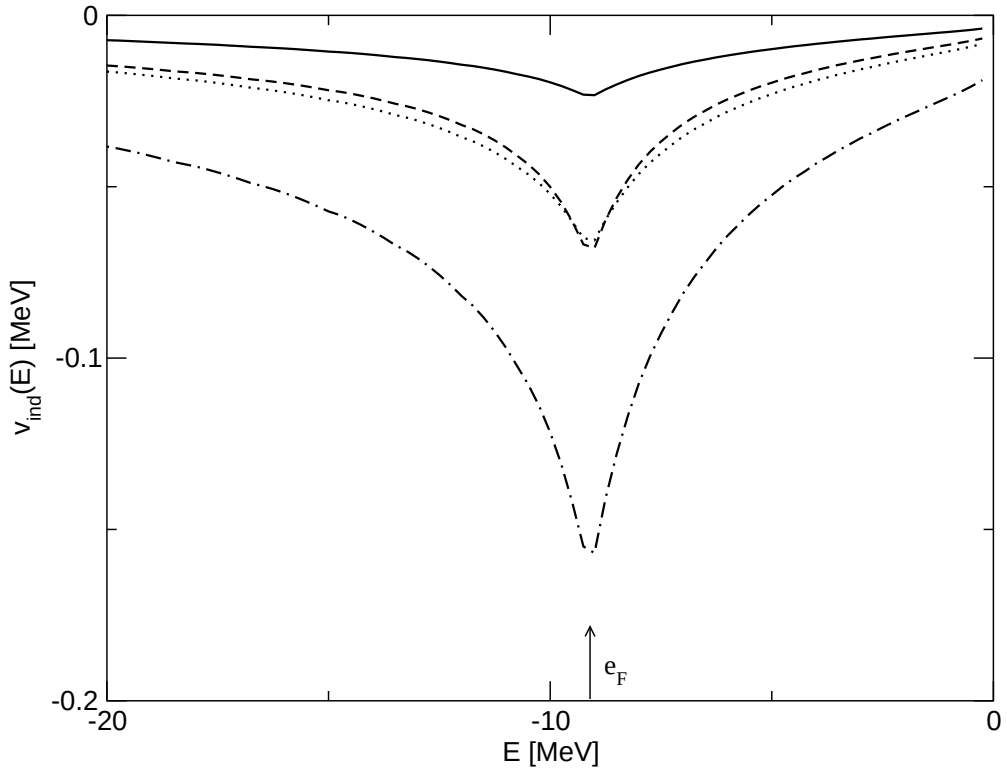

Figure 6: The nucleus ^{120}Sn. The semiclassical matrix elements of the induced interaction, as a function of the energy of the single-particle levels (calculated with $m_k = m$) associated with the multipolarities $L = 2$, 3, and 4 of the formfactor (see Eq.(1)), are shown by a dashed, dotted and solid line respectively. The sum of the three contributions is displayed by means of a dash-dotted line (cf. Fig. 5).

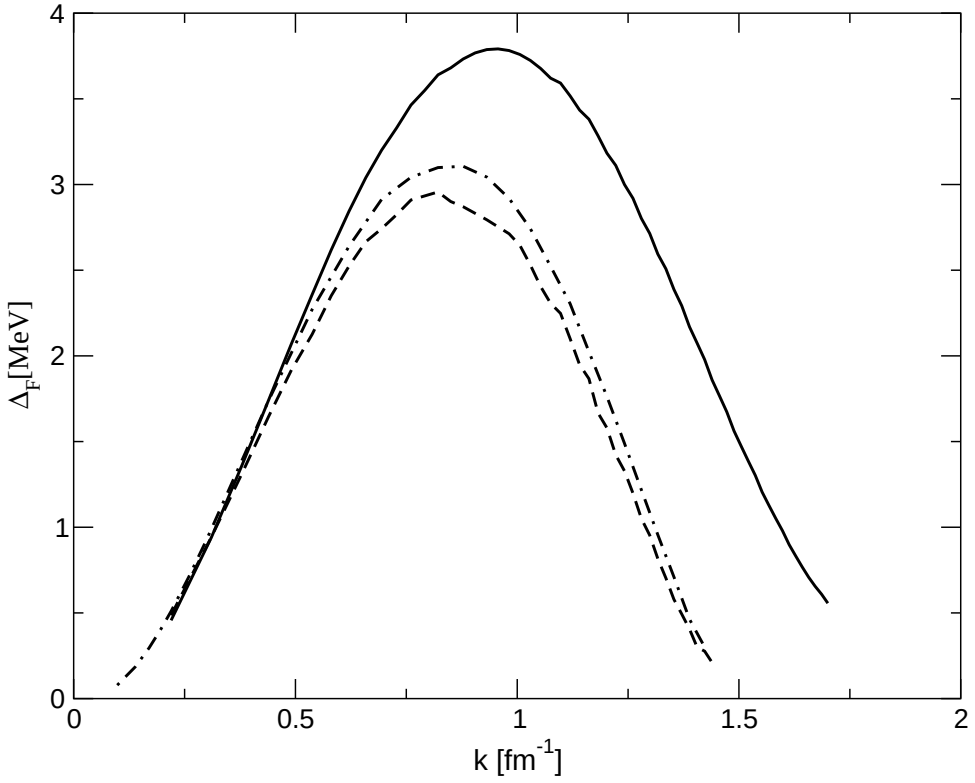

Figure 7: Pairing gaps calculated in neutron matter as a function of the Fermi momentum, obtained with the Gogny interaction (solid line), the Argonne v_{14} potential (dash-dotted line) and the v_{low-k} potential (dashed line). The bare effective mass has been used in the calculation.

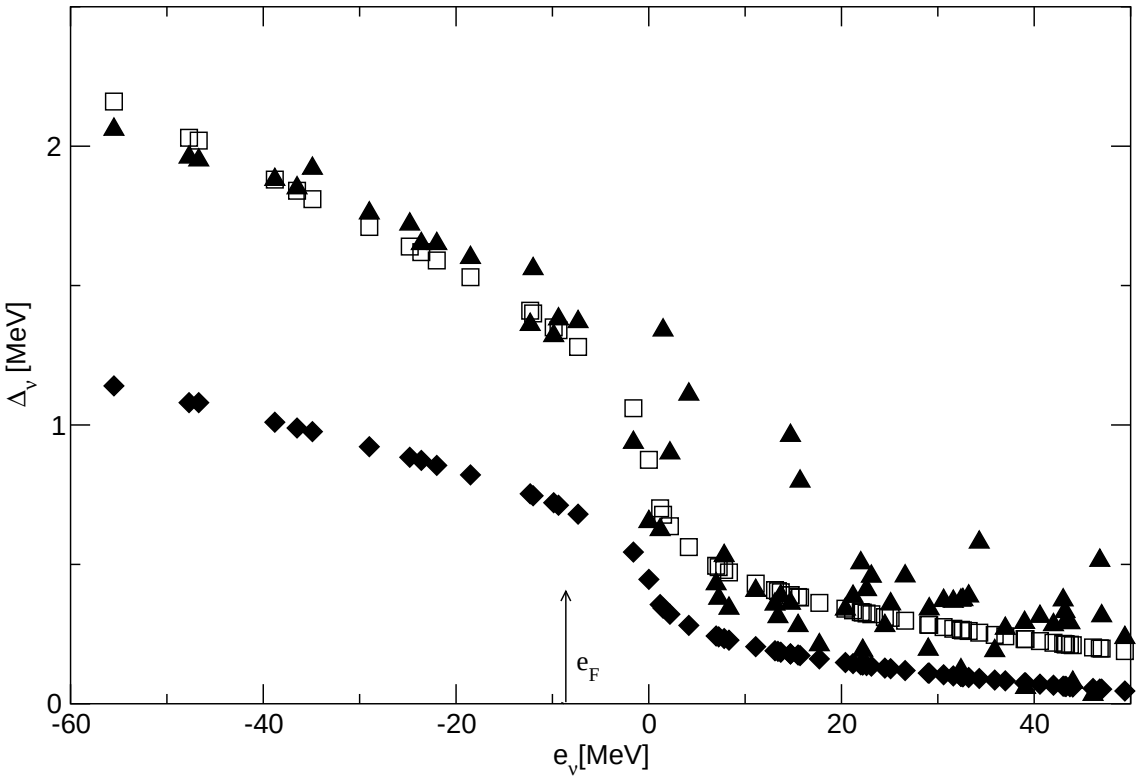

Figure 8: State-dependent pairing gaps of ^{120}Sn calculated with a Woods-Saxon potential (with depth V_0 = -64 MeV, diffusivity $a = 0.65$ fm and radius $R_0 = 6.17$ fm), as a function of the single-particle energy. The $k-$mass m_k was set equal to $0.7m$. The Fermi energy is e_F =- 8.6 MeV. Solid triangles (open squares) display the results of a HFB calculation with the Gogny interaction, with quantal (semiclassical) matrix elements. The solid diamonds refer instead to a HFB calculation using the semiclassical matrix elements of the v_{low-k} potential.

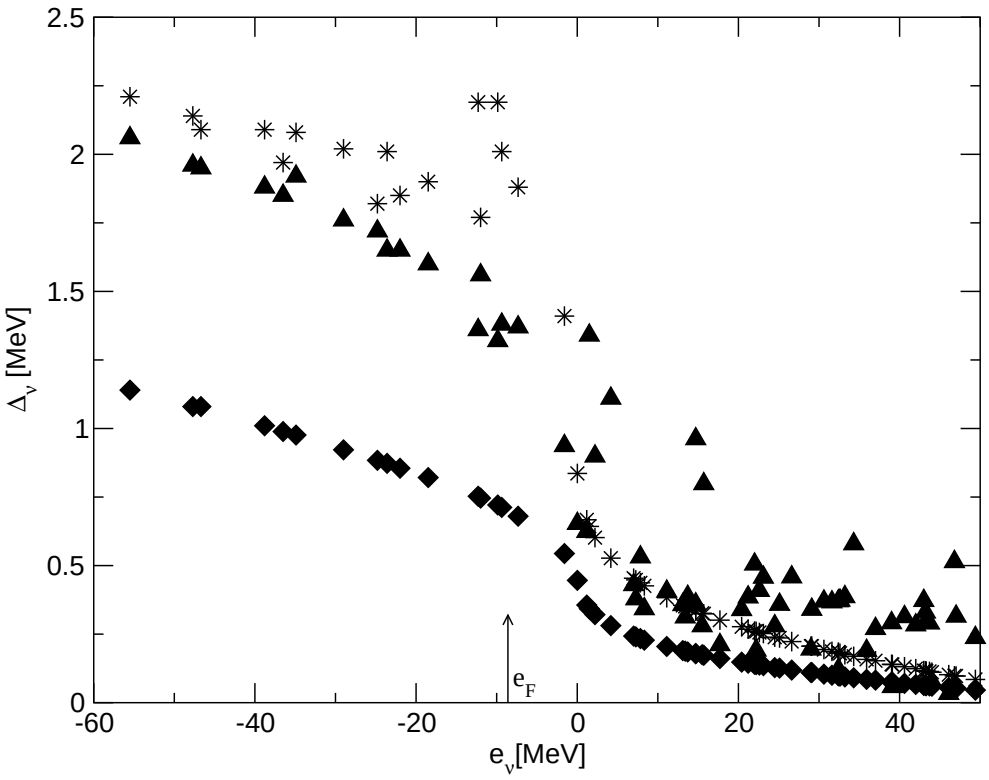

Figure 9: State-dependent pairing gap of ^{120}Sn obtained making use of the Woods-Saxon potential used in calculating the results displayed in Fig. 8 (i.e. with $m_k = 0.7m$) and different interactions. Diamonds and triangles show again the gaps obtained with the v_{low-k} and v_{Gogny} interactions, respectively. Stars show the gap associated with the matrix elements obtained summing the matrix elements of v_{low-k} and v_{ind}. The latter have been evaluated using Eqs. (9) and (10)

.